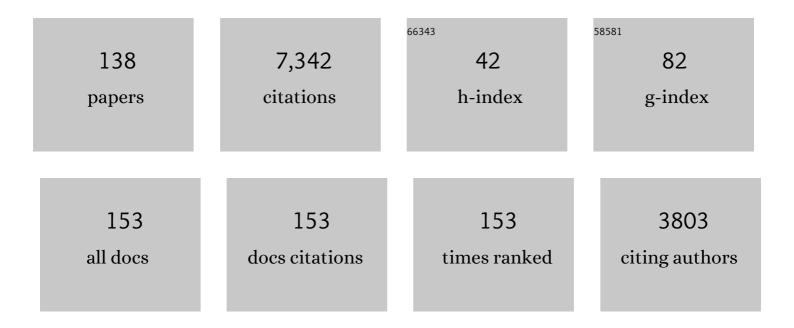
## Javier Escartin

List of Publications by Year in descending order

Source: https://exaly.com/author-pdf/4031690/publications.pdf Version: 2024-02-01



#	Article	IF	CITATIONS
1	Geochemistry of serpentinized and multiphase altered Atlantis Massif peridotites (IODP Expedition) Tj ETQq1 1 C 594, 120681.	).784314 3.3	rgBT /Overloo 9
2	SANTORY: SANTORiniâ $\in$ Ms Seafloor Volcanic ObservatorY. Frontiers in Marine Science, 2022, 9, .	2.5	6
3	Tectonic termination of oceanic detachment faults, with constraints on tectonic uplift and mass wasting related erosion rates. Earth and Planetary Science Letters, 2022, 584, 117449.	4.4	5
4	Effects of Substrate Composition and Subsurface Fluid Pathways on the Geochemistry of Seafloor Hydrothermal Deposits at the Lucky Strike Vent Field, Midâ€Atlantic Ridge. Geochemistry, Geophysics, Geosystems, 2022, 23, .	2.5	3
5	Integrating Multidisciplinary Observations in Vent Environments (IMOVE): Decadal Progress in Deep-Sea Observatories at Hydrothermal Vents. Frontiers in Marine Science, 2022, 9, .	2.5	5
6	Age and Rate of Accumulation of Metalâ€Rich Hydrothermal Deposits on the Seafloor: The Lucky Strike Vent Field, Midâ€Atlantic Ridge. Journal of Geophysical Research: Solid Earth, 2022, 127, .	3.4	4
7	K-Ar Geochronology and geochemistry of underwater lava samples from the Subsaintes cruise offshore Les Saintes (Guadeloupe): Insights for the Lesser Antilles arc magmatism. Marine Geology, 2022, 450, 106862.	2.1	3
8	Fluid Circulation Along an Oceanic Detachment Fault: Insights From Fluid Inclusions in Silicified Brecciated Fault Rocks (Midâ€Atlantic Ridge at 13°20′N). Geochemistry, Geophysics, Geosystems, 2021, 22	, 2.5	5
9	Quantification of Gravitational Mass Wasting and Controls on Submarine Scarp Morphology Along the Roseau Fault, Lesser Antilles. Journal of Geophysical Research F: Earth Surface, 2021, 126, e2020JF005892.	2.8	4
10	Co-seismic and post-seismic deformation, field observations and fault model of the 30 October 2020 Mw = 7.0 Samos earthquake, Aegean Sea. Acta Geophysica, 2021, 69, 999-1024.	2.0	28
11	Shallow-water hydrothermalism at Milos (Greece): Nature, distribution, heat fluxes and impact on ecosystems. Marine Geology, 2021, 438, 106521.	2.1	6
12	Radioactivity Monitoring in Ocean Ecosystems (RAMONES). , 2021, , .		3
13	Mid-Ocean Ridges and Their Geomorphological Features. , 2021, , .		2
14	Extrusive upper crust formation at slow-spreading ridges: Fault steering of lava flows. Earth and Planetary Science Letters, 2021, 576, 117202.	4.4	2
15	Deep oceanic submarine fieldwork with undergraduate students: an immersive experience with the Minerve software. Solid Earth, 2021, 12, 2789-2802.	2.8	5
16	Automatic scale estimation of structure from motion based 3D models using laser scalers in underwater scenarios. ISPRS Journal of Photogrammetry and Remote Sensing, 2020, 159, 13-25.	11.1	24
17	Origin of oceanic ferrodiorites by injection of nelsonitic melts in gabbros at the Vema Lithospheric Section, Mid Atlantic Ridge. Lithos, 2020, 368-369, 105589.	1.4	11
18	Fault Stability Across the Seismogenic Zone. Journal of Geophysical Research: Solid Earth, 2020, 125, e2020JB019670.	3.4	13

#	Article	IF	CITATIONS
19	Simulation of the 2004 tsunami of Les Saintes in Guadeloupe (Lesser Antilles) using new source constraints. Natural Hazards, 2020, 103, 2103-2129.	3.4	5
20	Terrestrial shallow water hydrothermal outflow characterized from out of space. Marine Geology, 2020, 422, 106119.	2.1	5
21	Chemical Mass Balance, Depositional Efficiency, and Rates of Formation of Seafloor Massive Sulfide Deposits. , 2020, , .		0
22	Investigating Fineâ€5cale Permeability Structure and Its Control on Hydrothermal Activity Along a Fastâ€5preading Ridge (the East Pacific Rise, 9°43â€2–53â€2N) Using Seismic Velocity, Poroelastic Response, Numerical Modeling. Geophysical Research Letters, 2019, 46, 11799-11810.	and	9
23	Performing submarine field survey without scuba gear using GIS-like mapping in a Virtual Reality environment. , 2019, , .		4
24	Scale Accuracy Evaluation of Image-Based 3D Reconstruction Strategies Using Laser Photogrammetry. Remote Sensing, 2019, 11, 2093.	4.0	12
25	Seafloor expression of oceanic detachment faulting reflects gradients in mid-ocean ridge magma supply. Earth and Planetary Science Letters, 2019, 516, 176-189.	4.4	25
26	Machine Tools Anomaly Detection Through Nearly Real-Time Data Analysis. Journal of Manufacturing and Materials Processing, 2019, 3, 97.	2.2	6
27	Simulation of the 2004 tsunami of Les Saintes in Guadeloupe (Lesser Antilles). , 2019, , .		3
28	Controls on the seafloor exposure of detachment fault surfaces. Earth and Planetary Science Letters, 2019, 506, 381-387.	4.4	13
29	Rifting Processes at a Continentâ€Ocean Transition Rift Revealed by Fault Analysis: Example of Dabbahuâ€Mandaâ€Hararo Rift (Ethiopia). Tectonics, 2019, 38, 190-214.	2.8	6
30	Jet Instability over Smooth, Corrugated, and Realistic Bathymetry. Journal of Physical Oceanography, 2019, 49, 585-605.	1.7	24
31	Frictional Heating Processes and Energy Budget During Laboratory Earthquakes. Geophysical Research Letters, 2018, 45, 12,274.	4.0	31
32	Ore component mobility, transport and mineralization at mid-oceanic ridges: A stable isotopes (Zn, Cu) Tj ETQq0 ( 2018, 503, 170-180.	) 0 rgBT /C 4.4	Overlock 10 29
33	Magmatism, serpentinization and life: Insights through drilling the Atlantis Massif (IODP Expedition) Tj ETQq1 1 0.	784314 rg 1.4	gðð /Overlo
34	Alteration Heterogeneities in Peridotites Exhumed on the Southern Wall of the Atlantis Massif (IODP) Tj ETQq0 0 (	).rgBT /Ov 2.8	eglock 10 T
35	Genesis of corrugated fault surfaces by strain localization recorded at oceanic detachments. Earth and Planetary Science Letters, 2018, 498, 116-128.	4.4	29

Tectonic structure, evolution, and the nature of oceanic core complexes and their detachment fault zones (13Ű20′N and 13Ű30′N, Mid Atlantic Ridge). Geochemistry, Geophysics, Geosystems, 2017, 18, 1451-1482.

#	Article	IF	CITATIONS
37	Pervasive silicification and hanging wall overplating along the 13°20′N oceanic detachment fault ( <scp>M</scp> idâ€ <scp>A</scp> tlantic <scp>R</scp> idge). Geochemistry, Geophysics, Geosystems, 2017, 18, 2028-2053.	2.5	21
38	An integrated view of the methane system in the pockmarks at Vestnesa Ridge, 79°N. Marine Geology, 2017, 390, 282-300.	2.1	74
39	Seismic Signatures of Hydrothermal Pathways Along the East Pacific Rise Between 9°16′ and 9°56′N. Journal of Geophysical Research: Solid Earth, 2017, 122, 10,241.	3.4	16
40	Oceanographic Signatures and Pressure Monitoring of Seafloor Vertical Deformation in Near-coastal, Shallow Water Areas: A Case Study from Santorini Caldera. Marine Geodesy, 2016, 39, 401-421.	2.0	5
41	Crustal accretion at a sedimented spreading center in the Andaman Sea. Geology, 2016, 44, 351-354.	4.4	22
42	Magnetic signatures of serpentinization at ophiolite complexes. Geochemistry, Geophysics, Geosystems, 2016, 17, 2969-2986.	2.5	44
43	Magmatic and tectonic extension at the Chile Ridge: Evidence for mantle controls on ridge segmentation. Geochemistry, Geophysics, Geosystems, 2016, 17, 2354-2373.	2.5	28
44	Dependence of seismic coupling on normal fault style along the <scp>N</scp> orthern <scp>M</scp> idâ€ <scp>A</scp> tlantic <scp>R</scp> idge. Geochemistry, Geophysics, Geosystems, 2016, 17, 4128-4152.	2.5	30
45	First direct observation of coseismic slip and seafloor rupture along a submarine normal fault and implications for fault slip history. Earth and Planetary Science Letters, 2016, 450, 96-107.	4.4	21
46	Response to Comment on "Sensitivity of seafloor bathymetry to climate-driven fluctuations in mid-ocean ridge magma supply― Science, 2016, 353, 229-229.	12.6	3
47	Response to Comment on "Sensitivity of seafloor bathymetry to climate-driven fluctuations in mid-ocean ridge magma supplyâ€, Science, 2016, 352, 1405-1405.	12.6	9
48	Tectonic evolution of 200 km of <scp>M</scp> idâ€ <scp>A</scp> tlantic <scp>R</scp> idge over 10 million years: Interplay of volcanism and faulting. Geochemistry, Geophysics, Geosystems, 2015, 16, 2303-2321.	2.5	26
49	Magmatic plumbing at Lucky Strike volcano based on olivineâ€hosted melt inclusion compositions. Geochemistry, Geophysics, Geosystems, 2015, 16, 126-147.	2.5	30
50	Threeâ€dimensional geometry of axial magma chamber roof and faults at Lucky Strike volcano on the Midâ€Atlantic Ridge. Journal of Geophysical Research: Solid Earth, 2015, 120, 5379-5400.	3.4	23
51	The Kallisti Limnes, carbon dioxide-accumulating subsea pools. Scientific Reports, 2015, 5, 12152.	3.3	18
52	Deformation mechanisms of antigorite serpentinite at subduction zone conditions determined from experimentally and naturally deformed rocks. Earth and Planetary Science Letters, 2015, 411, 229-240.	4.4	39
53	Sensitivity of seafloor bathymetry to climate-driven fluctuations in mid-ocean ridge magma supply. Science, 2015, 350, 310-313.	12.6	65
54	Hydrothermal activity along the slow-spreading Lucky Strike ridge segment (Mid-Atlantic Ridge): Distribution, heatflux, and geological controls. Earth and Planetary Science Letters, 2015, 431, 173-185.	4.4	32

#	Article	IF	CITATIONS
55	Permeability of the Lucky Strike deep-sea hydrothermal system: Constraints from the poroelastic response to ocean tidal loading. Earth and Planetary Science Letters, 2014, 408, 146-154.	4.4	13
56	Temporal variability and tidal modulation of hydrothermal exitâ€fluid temperatures at the Lucky Strike deepâ€sea vent field, Midâ€Atlantic Ridge. Journal of Geophysical Research: Solid Earth, 2014, 119, 2543-2566.	3.4	69
57	Lucky Strike seamount: Implications for the emplacement and rifting of segmentâ€centered volcanoes at slow spreading midâ€ocean ridges. Geochemistry, Geophysics, Geosystems, 2014, 15, 4157-4179.	2.5	22
58	Tectonic structure, lithology, and hydrothermal signature of the Rainbow massif (Mid-Atlantic Ridge) Tj ETQq0 0 0	rgBT /Ovo 2.5	erlock 10 Tf
59	Alongâ€axis hydrothermal flow at the axis of slow spreading Midâ€Ocean Ridges: Insights from numerical models of the Lucky Strike vent field (MAR). Geochemistry, Geophysics, Geosystems, 2014, 15, 2918-2931.	2.5	15
60	Hydrothermal seismicity beneath the summit of Lucky Strike volcano, Mid-Atlantic Ridge. Earth and Planetary Science Letters, 2013, 373, 118-128.	4.4	27
61	Atypically depleted upper mantle component revealed by Hf isotopes at Lucky Strike segment. Chemical Geology, 2013, 341, 128-139.	3.3	29
62	Optical methods to monitor temporal changes at the seafloor: The Lucky Strike deep-sea hydrothermal vent field (Mid-Atlantic Ridge). , 2013, , .		3
63	Mapping the Moon: Using a lightweight AUV to survey the site of the 17th century ship â€ <sup>-</sup> La Lune'. , 2013, ,		42
64	Automated classification and thematic mapping of bacterial mats in the North Sea. , 2013, , .		11
65	A Novel Blending Technique for Underwater Gigamosaicing. IEEE Journal of Oceanic Engineering, 2012, 37, 626-644.	3.8	49
66	Structure, temporal evolution, and heat flux estimates from the Lucky Strike deepâ€sea hydrothermal field derived from seafloor image mosaics. Geochemistry, Geophysics, Geosystems, 2012, 13, .	2.5	71
67	Quantifying diffuse and discrete venting at the Tour Eiffel vent site, Lucky Strike hydrothermal field. Geochemistry, Geophysics, Geosystems, 2012, 13, .	2.5	47
68	Deformation associated with the denudation of mantleâ€derived rocks at the Midâ€Atlantic Ridge 13°–15°N: The role of magmatic injections and hydrothermal alteration. Geochemistry, Geophysics, Geosystems, 2012, 13, .	2.5	38
69	Active Long-Lived Faults Emerging Along Slow-Spreading Mid-Ocean Ridges. Oceanography, 2012, 25, 94-99.	1.0	21
70	Challenges of close-range underwater optical mapping. , 2011, , .		3
71	Drilling constraints on lithospheric accretion and evolution at Atlantis Massif, Mid-Atlantic Ridge 30°N. Journal of Geophysical Research, 2011, 116, .	3.3	112
72	Detachments in Oceanic Lithosphere: Deformation, Magmatism, Fluid Flow, and Ecosystems. Eos, 2011, 92, 31-31.	0.1	77

#	Article	IF	CITATIONS
73	Quantitative constraint on footwall rotations at the 15°45′N oceanic core complex, Midâ€Atlantic Ridge: Implications for oceanic detachment fault processes. Geochemistry, Geophysics, Geosystems, 2011, 12, .	2.5	43
74	Rare gas systematics on Lucky Strike basalts (37°N, North Atlantic): Evidence for efficient homogenization in a long-lived magma chamber system?. Geophysical Research Letters, 2011, 38, n/a-n/a.	4.0	18
75	Hydrothermally-induced melt lens cooling and segmentation along the axis of fast- and intermediate-spreading centers. Geophysical Research Letters, 2011, 38, n/a-n/a.	4.0	25
76	Regional seismicity of the Mid-Atlantic Ridge: observations from autonomous hydrophone arrays. Geophysical Journal International, 2010, 183, 1559-1578.	2.4	30
77	Tectonic versus magmatic extension in the presence of core complexes at slow-spreading ridges from a visualization of faulted seafloor topography. Geology, 2010, 38, 615-618.	4.4	49
78	Upper crustal velocity structure beneath the central Lucky Strike Segment from seismic refraction measurements. Geochemistry, Geophysics, Geosystems, 2010, 11, .	2.5	27
79	A noninvasive method for measuring the velocity of diffuse hydrothermal flow by tracking moving refractive index anomalies. Geochemistry, Geophysics, Geosystems, 2010, 11, .	2.5	12
80	A short electromagnetic profile across the Kane Oceanic Core Complex. Geophysical Research Letters, 2010, 37, .	4.0	6
81	Serpentinization and associated hydrogen and methane fluxes at slow spreading ridges. Geophysical Monograph Series, 2010, , 241-264.	0.1	83
82	Seismological constraints on the thermal structure along the Lucky Strike segment (Mid-Atlantic) Tj ETQq0 0 0 rg Geophysical Researches, 2009, 30, 105-120.	BT /Overlo 1.2	ock 10 Tf 50 20
83	Oceanic corrugated surfaces and the strength of the axial lithosphere at slow spreading ridges. Earth and Planetary Science Letters, 2009, 288, 174-183.	4.4	59
84	A record of eruption and intrusion at a fast spreading ridge axis: Axial summit trough of the East Pacific Rise at 9–10°N. Geochemistry, Geophysics, Geosystems, 2009, 10, .	2.5	44
85	Central role of detachment faults in accretion of slow-spreading oceanic lithosphere. Nature, 2008, 455, 790-794.	27.8	407
86	Fault rotation and core complex formation: Significant processes in seafloor formation at slowâ€spreading midâ€ocean ridges (Midâ€Atlantic Ridge, 13°–15°N). Geochemistry, Geophysics, Geosyster 2008, 9, .	m <b>2,</b> 5	186
87	Globally aligned photomosaic of the Lucky Strike hydrothermal vent field (Midâ€Atlantic Ridge,) Tj ETQq1 1 0.784 Geophysics, Geosystems, 2008, 9, .	314 rgBT 2.5	/Overlock 1 56
88	Relationships between the microstructural evolution and the rheology of talc at elevated pressures and temperatures. Earth and Planetary Science Letters, 2008, 268, 463-475.	4.4	105
89	Mechanical decoupling and thermal structure at the East Pacific Rise axis 9°N: Constraints from axial magma chamber geometry and seafloor structures. Earth and Planetary Science Letters, 2008, 272, 19-28.	4.4	16
90	Hydration due to high-T brittle failure within in situ oceanic crust, 30°N Mid-Atlantic Ridge. Earth and Planetary Science Letters, 2008, 275, 348-354.	4.4	22

#	Article	IF	CITATIONS
91	Automated quantification of gradient defined features. , 2008, , .		Ο
92	Hydrothermal circulation at slow-spreading mid-ocean ridges: The role of along-axis variations in axial lithospheric thickness. Geology, 2008, 36, 759.	4.4	28
93	Oceanic core complexes and crustal accretion at slow-spreading ridges. Geology, 2007, 35, 623.	4.4	302
94	80-Myr history of buoyancy and volcanic fluxes along the trails of the Walvis and St. Helena hotspots (South Atlantic). Earth and Planetary Science Letters, 2007, 261, 432-442.	4.4	30
95	Seismic and magnetic anisotropy of serpentinized ophiolite: Implications for oceanic spreading rate dependent anisotropy. Earth and Planetary Science Letters, 2007, 261, 590-601.	4.4	14
96	Oceanic detachment faults focus very large volumes of black smoker fluids. Geology, 2007, 35, 935.	4.4	205
97	Interplay between faults and lava flows in construction of the upper oceanic crust: The East Pacific Rise crest 9°25′-9°58′N. Geochemistry, Geophysics, Geosystems, 2007, 8, n/a-n/a.	2.5	54
98	Monitoring and Observatories: Multidisciplinary, Time-Series Observations at Mid-Ocean Ridges. Oceanography, 2007, 20, 128-137.	1.0	5
99	Dynamic control on serpentine crystallization in veins: Constraints on hydration processes in oceanic peridotites. Geochemistry, Geophysics, Geosystems, 2007, 8, n/a-n/a.	2.5	187
100	Heat flow variations on a slowly accreting ridge: Constraints on the hydrothermal and conductive cooling for the Lucky Strike segment (Mid-Atlantic Ridge, 37°N). Geochemistry, Geophysics, Geosystems, 2006, 7, n/a-n/a.	2.5	15
101	Widespread active detachment faulting and core complex formation near 13° N on the Mid-Atlantic Ridge. Nature, 2006, 442, 440-443.	27.8	243
102	Discovery of a magma chamber and faults beneath a Mid-Atlantic Ridge hydrothermal field. Nature, 2006, 442, 1029-1032.	27.8	248
103	Modes of seafloor generation at a melt-poor ultraslow-spreading ridge. Geology, 2006, 34, 605.	4.4	337
104	IODP Expedition 304 & 305 Characterize the Lithology, Structure, and Alteration of an Oceanic Core Complex. Scientific Drilling, 2006, , .	0.6	13
105	Modes of seafloor generation at a melt-poor ultraslow-spreading ridge. Geology, 2006, 34, 605.	4.4	1
106	IODP Expeditions 304 and 305 - Oceanic Core Complex Formation, Atlantis Massif. Scientific Drilling, 2005, , .	0.6	1
107	Constraints on deformation conditions and the origin of oceanic detachments: The Mid-Atlantic Ridge core complex at 15°45′N. Geochemistry, Geophysics, Geosystems, 2003, 4, .	2.5	234
108	Spatial and temporal distribution of seismicity along the northern Mid-Atlantic Ridge (15°-35°N). Journal of Geophysical Research, 2003, 108, .	3.3	99

#	Article	IF	CITATIONS
109	Parallel bands of seismicity at the Mid-Atlantic Ridge, 12-14°N. Geophysical Research Letters, 2003, 30, .	4.0	23
110	Differing Views on Science in Spain. Science, 2003, 300, 51c-52.	12.6	2
111	Direct geologic evidence for oceanic detachment faulting: The Mid-Atlantic Ridge, 15°45′N: Comment and Reply. Geology, 2003, 31, e15-e15.	4.4	2
112	Direct geologic evidence for oceanic detachment faulting: The Mid-Atlantic Ridge, 15º45′N: Comment and Reply. Geology, 2003, 31, e14-e14.	4.4	1
113	Direct geological evidence for oceanic detachment faulting: The Mid-Atlantic Ridge, 15°45′N. Geology, 2002, 30, 879.	4.4	188
114	Focused volcanism and growth of a slow spreading segment (Mid-Atlantic Ridge, 35°N). Earth and Planetary Science Letters, 2001, 185, 211-224.	4.4	28
115	Strength of slightly serpentinized peridotites: Implications for the tectonics of oceanic lithosphere. Geology, 2001, 29, 1023.	4.4	280
116	Crustal thickness of V-shaped ridges south of the Azores: Interaction of the Mid-Atlantic Ridge (36°-39°N) and the Azores hot spot. Journal of Geophysical Research, 2001, 106, 21719-21735.	3.3	90
117	Extremely asymmetric magmatic accretion of oceanic crust at the ends of slow-spreading ridge segments. Geology, 2000, 28, 179.	4.4	49
118	Seismic structure across the rift valley of the Mid-Atlantic Ridge at 23°20′ (MARK area): Implications for crustal accretion processes at slow spreading ridges. Journal of Geophysical Research, 2000, 105, 28411-28425.	3.3	98
119	Extremely asymmetric magmatic accretion of oceanic crust at the ends of slow-spreading ridge segments. Geology, 2000, 28, 179-182.	4.4	1
120	Spanish recruitment openly favours insiders. Nature, 1999, 401, 112-112.	27.8	2
121	Ultramafic exposures and the gravity signature of the lithosphere near the Fifteen-Twenty Fracture Zone (Mid-Atlantic Ridge, 14°–16.5ŰN). Earth and Planetary Science Letters, 1999, 171, 411-424.	4.4	90
122	Mid-Atlantic Ridge–Azores hotspot interactions: along-axis migration of a hotspot-derived event of enhanced magmatism 10 to 4 Ma ago. Earth and Planetary Science Letters, 1999, 173, 257-269.	4.4	190
123	Quantifying tectonic strain and magmatic accretion at a slow spreading ridge segment, Mid-Atlantic Ridge, 29°N. Journal of Geophysical Research, 1999, 104, 10421-10437.	3.3	83
124	Toxic spill caught Spain off guard. Nature, 1998, 395, 110-110.	27.8	5
125	Sedimentation on young ocean floor at the Mid-Atlantic Ridge, 29 °N. Marine Geology, 1998, 148, 1-8.	2.1	15
126	Fault structure and detailed evolution of a slow spreading ridge segment: the Mid-Atlantic Ridge at 29°N. Earth and Planetary Science Letters, 1998, 154, 167-183.	4.4	55

#	Article	IF	CITATIONS
127	Detachment faults at mid-ocean ridges garner interest. Eos, 1998, 79, 127-127.	0.1	29
128	Effects of serpentinization on the lithospheric strength and the style of normal faulting at slow-spreading ridges. Earth and Planetary Science Letters, 1997, 151, 181-189.	4.4	225
129	Nondilatant brittle deformation of serpentinites: Implications for Mohr-Coulomb theory and the strength of faults. Journal of Geophysical Research, 1997, 102, 2897-2913.	3.3	203
130	Corrugated slip surfaces formed at ridge–transform intersections on the Mid-Atlantic Ridge. Nature, 1997, 385, 329-332.	27.8	453
131	Flow Structure and Dispersion within Algal Mats. Estuarine, Coastal and Shelf Science, 1995, 40, 451-472.	2.1	48
132	Ridge offsets, normal faulting, and gravity anomalies of slow spreading ridges. Journal of Geophysical Research, 1995, 100, 6163-6177.	3.3	66
133	The Rheology and Morphology of Oceanic Lithosphere and Mid-Ocean Ridges. Geophysical Monograph Series, 0, , 63-93.	0.1	18
134	The Rheology of the Lower Oceanic Crust: Implications for Lithospheric Deformation at Mid-Ocean Ridges. Geophysical Monograph Series, 0, , 291-303.	0.1	56
135	Expedition 357 summary. Proceedings of the International Ocean Discovery Program, 0, , .	0.0	16
136	Expedition 357 methods. Proceedings of the International Ocean Discovery Program, 0, , .	0.0	11
137	Fault responsible for Samos earthquake identified. Temblor, 0, , .	0.0	24
138	New insights into the plumbing system of Santorini using helium and carbon isotopes. Geochemical Perspectives Letters, 0, , 46-50.	5.0	3